Effects of Nonlinearity on Wave-Induced Fluid Resonance within A Narrow Gap Between Two Barges

Zhiwei SONG[1], Lin LU[1,2,*], Guoqiang TANG[1,2], Xiaofan LOU[1,2] and Liang CHENG[1,2,3]
[1]State Key Laboratory of Coastal and Offshore Engineering, Dalian University of Technology, Dalian, China
[2]International Joint Laboratory on Offshore Oil & Gas Engineering, Dalian University of Technology, Dalian, China
[3]School of Engineering, The University of Western Australia, Crawley 6009, Australia
[*]Lulin@dlut.edu.cn

HIGHLIGHTS

- Effects of free surface nonlinearity on the fluid resonance within a narrow gap are quantified.
- The nonlinear Duffing oscillator feature, namely, the soften/harden spring dynamics, is demonstrated, and is resulted from the second order effect with a rise of the mean water level.
- Due to the quadratic and cubic nonlinearity, super-harmonic resonance and combined harmonic resonance are obtained.
- Nonlinear hydrodynamics, such as co-exiting periodic motions (Period 2 motion, Period 3 motion) and higher order harmonic components, are studied.

1 INTRODUCTION

Fluid resonance in a narrow gap, or gap resonance, has received extensive attentions on account of extremely large response amplitudes in the gap may be excited for two vessels with side-by-side arrangement (Molin, 2001; Kristiansen and Faltinsen, 2008; Lu et. al, 2010, 2011; Feng and Bai, 2015). Previous studies have shown that the wave response amplitudes around the resonant frequencies (ω_R) are generally over-predicted by the linear potential flow theory, due to the damping effect (Kristiansen and Faltinsen, 2008; Lu et. al, 2010) or the nonlinearity (Kristiansen and Faltinsen, 2008; Feng and Bai, 2015). Based on the relatively smaller wave steepness or forced amplitudes, both Kristiansen and Faltinsen (2008) and Feng and Bai (2015) concluded that the nonlinearity effect was insignificant in suppressing resonance responses. However, effects of nonlinearity on the responses around the primary resonant frequency were not quantified. Apart from the primary resonance around the first-order resonant frequency, a secondary resonance, i.e. the second order resonance, has been observed by Li (2019) as well. The second order resonance describes a local extreme response amplitude when the forcing frequency is close to half of resonant frequency $\omega_R/2$, which results from second-order harmonic components. Hence, it can be speculated that the nonlinearity plays a major role in the response at around half of the primary resonant frequencies.

In the present paper, the wave-induced fluid resonance in a narrow gap between two barges is investigated. Firstly, effects of the free surface nonlinearity on the fluid resonance within a narrow gap are quantified based on previous experimental and present numerical results. Then the nonlinear Duffing oscillator feature, namely, the soften/harden spring dynamics, is demonstrated for various incident wave amplitudes. A further investigation confirms that the nonlinear Duffing behavior results from the second order effect with a rise of the mean water level. Considering a nonlinear oscillator with quadratic or cubic nonlinearity, the secondary resonance is investigated within a wide range of incident wave frequency $\omega \in [0.29\omega_R, 1.48\omega_R]$. Finally, the nonlinear hydrodynamics, such as co-exiting periodic motions, are discussed based on phase portraits and amplitude spectrums.

2 NUMERICAL MODELS

The schematic diagram of the present numerical wave flume is demonstrated in Fig. 1. The origin of a Cartesian coordinate system *O-xy* is at the mean water free surface with the positive *x*-axis in the propagation direction of the incident wave and the positive *y*-axis being vertically upwards. As shown in Fig. 1, two boxes are firmly fixed in the numerical wave flume. With respect to the incoming wave direction, Barge 1 is the leading barge, and has a breadth B_1 and a draft d_1. The breadth and draft of Barge 2 are defined as B_2, and d_2, respectively. The narrow gap between Barge 1 and Barge 2 has a width B_g. Six wave gauges are employed to record the wave surface elevation. Hereafter, the wave surface elevation measured by wave gauge G_p is labelled by η_p (p = 1, 2, 3, 4, 5 and 6) and the corresponding wave height and wave amplitude are denoted by H_p and A_p, respectively.

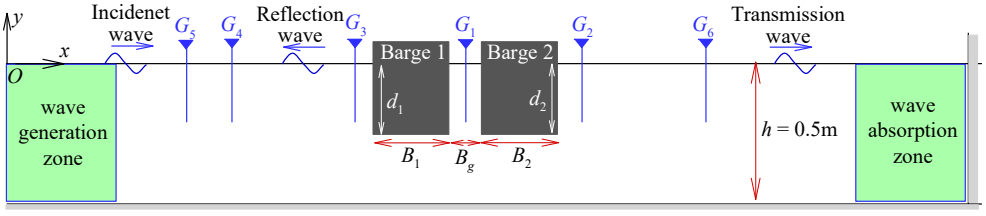

FIGURE 1. Schematic diagram of the numerical wave flume and the definition of the coordinate system.

To investigate the effect of the free surface nonlinearity on the wave-induced fluid response within a narrow gap, a fully nonlinear time domain model and a linear time domain model are developed. Both two numerical wave models are established based on potential flow theory. The finite element method (FEM) is employed to discretize the whole fluid domain. At the beginning of the simulation, a ramp function is applied to prevent the impulse-like solution and to reduce the transient waves. A relaxation zone method developed by Jacobsen, Fuhrman and Fredsøe (2012) is employed to eliminate the wave reflection. To generate the designed incident waves, the theoretical velocity potential is specified at the inlet boundary, where the Airy wave is adopted in the linear model and fifth-order Stokes wave (Fenton,1985) is given in the fully nonlinear model. In order to satisfy the fully nonlinear boundary conditions at the instantaneous free surface in the fully nonlinear model, moving grid method in Arbitrary-Lagrangian-Eulerian Frame (Donea, Giuliani, and Halleux, 1982) is adopted here to track the free surface at each time step. Moreover, a Chebyshev 5-point smoothing scheme is employed in the fully nonlinear model to eliminate the saw-tooth numerical instabilities.

3 RESULTS AND DISCUSSIONS

Effects of the free surface nonlinearity in the fluid resonant response are firstly qualified based on the previous experimental results (Liu et al., 2016) and the present numerical results. The setup of numerical simulations is in accordance with that of the experiment, which is such that $B_1 = 0.20$m, $B_2 = 1.00$m, $d_1 = d_2 = 0.25$m and $B_g = 0.05$m. the water depth h is set as 0.50m and the incident wave height H is set as 0.03m. The range of the incident wave frequency ω is kept within [3.14rad/s, 7.85rad/s]. Variations of the non-dimensional average wave response height H_1/H with respect to the non-dimension incident wave frequency $\omega/(g/h)^{0.50}$ are demonstrated in Fig. 2 for the present and previous studies, where H_1 is the wave response height. The computation around the resonant frequency ω_R in the fully nonlinear flow model is collapsed because of overly distorted meshes induced by the extremely large amplitude of the response in gap. A noticeable feature of the results is that non-dimensional fully nonlinear response amplitude H_1/H is relatively smaller than that of the linear potential result when the incident wave frequency ω approaches the resonant frequency ω_R, which is induced by transfer of energy to higher modes owing to nonlinearities. Moreover, due to the nonlinear effect, an inclined trend in the distribution of H_1/H is observed around the resonant frequency in the fully nonlinear potential results, as denoted by the blue arrow line. While for the linear result, the distribution of H_1/H demonstrates a vertical trend as the incident wave frequency approaches the resonant frequency, as denoted by the black arrow line. Fig. 3 displays the amplitude difference values $\Delta_{l\text{-}f}$ between the linear response and the fully nonlinear response, as well as the amplitude difference values $\Delta_{l\text{-}e}$ between the linear result and the experimental result around the resonant frequency. The percentage $\Theta = \Delta_{l\text{-}f}/\Delta_{l\text{-}e}$ is defined to quantify the nonlinear effect, which means the nonlinear effects in suppressing the difference values between linear response and experimental response. From this figure, it can be seen that the value of Θ can reach 55% around the resonant frequency, which indicates that the free surface nonlinearity is of more significance than the damping effect in suppressing the difference between the linear response and the experimental one.

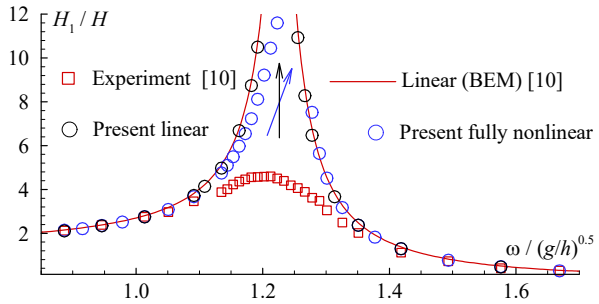

FIGURE 2. Variations of non-dimension wave response amplitude H_1/H with respect to non-dimensional incident wave frequency $\omega/(g/h)^{0.50}$, black arrow line ↑ and blue arrow line ↗ denote the trend of linear and fully nonlinear responses around the resonant frequency, respectively.

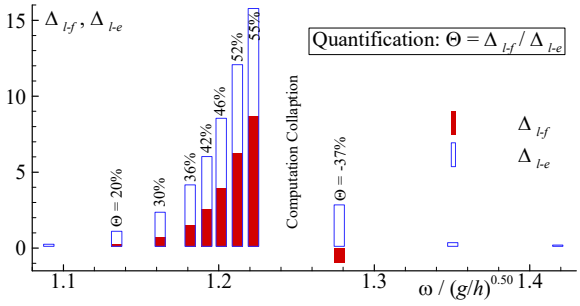

FIGURE 3. Quantification of free surface nonlinear effects on the fluid resonant response around the resonant frequency.

Wave-induced fluid oscillations in a single gap under different incident wave amplitudes are further examined to illustrate the effect of free surface nonlinearity on the nonlinear hydrodynamics. Hereafter, numerical setups are such that $B_1 = B_2 = 0.50$m, $d_1 = d_2 = 0.25$m, $B_g = 0.05$m, $h = 0.50$m, and four different incident wave amplitudes $H = 0.01$m, 0.02m, 0.03m and 0.04m. Both linear and fully nonlinear simulations are conducted in the time domain. Fig. 4 represents the amplitude-frequency responses for different incident wave amplitudes. All responses present a forward sweep, which is a typical feature of the nonlinear Duffing oscillator, namely, the harden spring dynamics. With the increase of the incident wave amplitude, the primary resonant frequency ω_R shifts towards the high frequency. Based on the harmonic analysis, the nonlinear Duffing behavior is found to result from the second order effect with a rise of the mean water level.

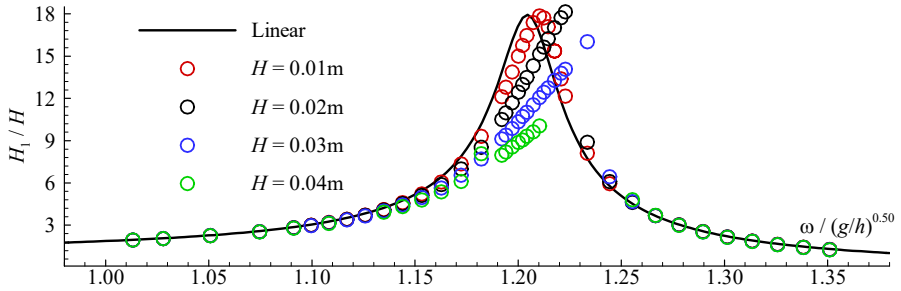

FIGURE 4. Variations of non-dimension wave response amplitudes H_1/H with respect to non-dimensional incident wave frequency $\omega/(g/h)^{0.50}$ under different incident wave amplitudes.

The nonlinear harden spring dynamics indicates the existence of the stiffness nonlinearity and moreover reflects the possibility of the secondary resonance. Therefore, a further simulation is carried out within a broader range of incident wave frequency $\omega \in [0.29\omega_R,\ 1.48\omega_R]$ at a constant wave height H = 0.04m. Results of both nonlinear and linear amplitude-frequency responses are presented in Fig. 5, where the response height H_1 is obtained by averaging the difference values between maximum and minimum in each period during 20 steady periods, as shown in the inset diagram of Fig. 5. The linear response presents a single peak in the response amplitude at $\omega = \omega_R$ = 5.32rad/s, whereas the nonlinear response demonstrates two more local peaks at $\omega = \omega_R/2$ and $\omega = \omega_R/3$, noted as **A** and **B**, respectively. Hence, except the primary resonance at $\omega = \omega_R$ = 5.32rad/s, super-harmonic resonance, a secondary resonance, is observed in the wave-induced fluid oscillations within a narrow gap. Next, combined harmonic resonance is investigated by introducing bi-chromatic incident waves with $\omega_I = \omega_R/4$, $\omega_{II} = 3\omega_R/4$, H_I = 0.04m and H_{II} = 0.04m. The time history of response and the corresponding amplitude spectrums at two different time intervals are shown in Fig. 6. It can be seen that response amplitude grows with respect to time. The amplitude spectrums indicate that the increase of the response at the sum-frequency, i.e. $\omega_I + \omega_{II} = \omega_R$, leads to the increase in the total response amplitudes, namely, the combined harmonic resonance. A further analysis shows that both the super-harmonic resonance and combined harmonic resonance are mainly attributed to the quadratic and cubic stiffness nonlinearities, which results from the second order effect with a rise of the mean water level.

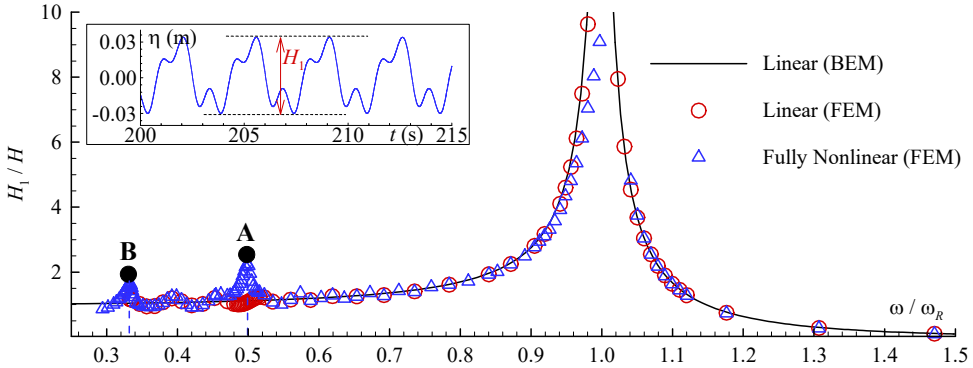

FIGURE 5. Variations of non-dimension wave response amplitude H_1/H with respect to non-dimensional incident wave frequency ω/ω_R. The inset figure illustrates the definition of the average response height H_1.

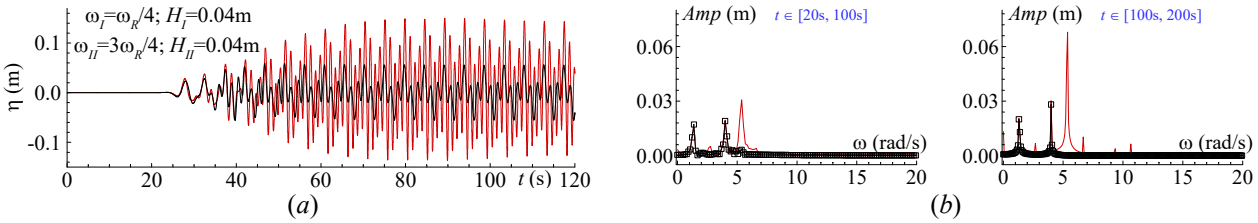

FIGURE 6. (*a*) Times histories of wave response in the single gap induced by bi-chromatic waves with $\omega_I = \omega_R/4$ and $\omega_{II} = 3\omega_R/4$. (*b*) Corresponding amplitude spectrums for two different time intervals.

The nonlinear behaviors of the above three extreme points are further examined for $\omega = 0.99\omega_R$, $\omega = \omega_R/2$, and $\omega = \omega_R/3$, in terms of the time history of the wave response, the amplitude spectrum and the phase portrait on the plane ($d\eta/dt$, η). Results are presented in Fig. 7. Firstly, differences in the time series of the wave response between the linear and the nonlinear response indicate that the free surface nonlinearity affects not only the response amplitude, but also the wave form, as two wave crests at $\omega_R/2$ and three wave crests at $\omega_R/3$ within a period have been observed. Hence, the higher order harmonics are motivated and determine the response amplitude. Secondly, the amplitude spectrum shows that the

second order response amplitude at $\omega_R/2$ is motivated and is higher than the first order response amplitude. At $\omega_R/3$, the third order response amplitude is motivated and the value is approximately equal to the first order response amplitude. Finally, the phase portrait indicates that the period 2 and period 3 motions exist in the response at $\omega = \omega_R/2$ and $\omega_R/3$, respectively.

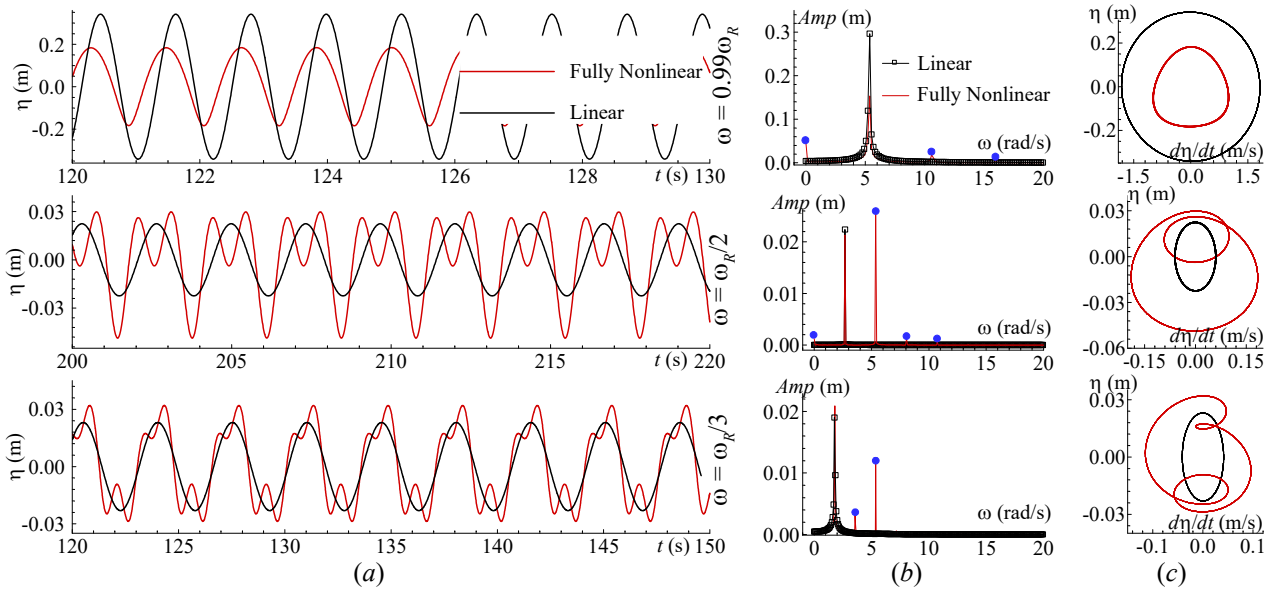

FIGURE 7. Time histories of the wave response in the gap, corresponding amplitude spectrums and phase portraits on the plane ($d\eta/dt$, η) for incident wave frequencies $\omega = 0.99\omega_R$, $\omega = \omega_R/2$, and $\omega = \omega_R/3$. The blue dot ● represents the extra higher order components in the fully nonlinear results compared with the linear response.

4 CONCLUSIONS

Effects of free surface nonlinearity on the fluid resonant response within a narrow gap between two barges are quantified. Results show that the nonlinearity is of more significance than the damping effect in suppressing the difference between the linear response and the experimental response around the resonant frequency. Harmonic analysis shows that the second order effect with a rise of the mean water level leads to the quadratic and cubic stiffness nonlinearity, which results in the nonlinear Duffing oscillator feature with harden spring dynamics, the existence of super-harmonic resonance and combined harmonic resonance, and the co-exiting periodic motions (Period 2 motion and Period 3 motion) in the fully nonlinear response.

ACKNOWLEDGEMETS

This work is supported by the National Natural Science Foundation of China with grant No. 51490673 and National Key R&D Program of China with grant No. 2016YFE0200100.

REFERENCES

[1] B. Molin, "On the piston and sloshing modes in moonpools," *J. Fluid Mech.*, 2001, 430, pp. 27-50.
[2] C. Liu, G. Tang, L. Lu, L. Tan, Z. Song, and Z. Zhou, "Experimental and numerical investigations of wave resonance in gap between two floating barges with various breadths," *Proc. 8th Chinese-German Joint Symp. on Hydraulic and Ocean Eng.*, Qingdao, China. 2016.
[3] J. D. Fenton, "A fifth-order Stokes theory for steady waves," *J. Waterway Port Coast.*, 1985, 111(2), pp. 216-234.
[4] J. Donea, S. Giuliani, and J. P. Halleux, "An arbitrary Lagrangian-Eulerian finite element method for transient dynamic fluid-structure interactions," *Comput. Method Appl. M.*, 1982, 33(1-3), pp. 689-723.
[5] L. Lu, B. Teng, L. Sun, and B. Chen, "Modelling of multi-bodies in close proximity under water waves—Fluid forces on floating bodies," *Ocean Eng.*, 2011, 38(13), pp. 1403-1416.
[6] L. Lu, L. Cheng, B. Teng, and M. Zhao, "Numerical investigation of fluid resonance in two narrow gaps of three identical rectangular structures," *Appl. Ocean Res.*, 2010, 32(2), pp. 177-190.
[7] N. G. Jacobsen, D. R. Fuhrman, and J. A. Fredsøe, "Wave generation toolbarge for the open-source CFD library: OpenFoam®," *Int. J. Numer. Meth. Fluids*, 2012, 70(9), pp. 1073-1088.
[8] T. Kristiansen, and O. M. Faltinsen, "Application of a vortex tracking method to the piston-like behaviour in a semi-entrained vertical gap," *Appl. Ocean Res.*, 2008, 30(1), pp. 1-16.
[9] X. Feng, and W. Bai, "Wave resonances in a narrow gap between two barges using fully nonlinear numerical simulation," *Appl. Ocean Res.*, 2015, 50, pp. 119-129.
[10] Y. Li, "Fully nonlinear analysis of second-order gap resonance between two floating barges," *Eng. Aanl. Bound. Elem.*, 2019, 106, pp. 1-19.